Proceedings of the ASME 2016 Fluids Engineering Division Summer Meeting
FEDSM2016
July 10-14, 2016, Washington, DC, USA

FEDSM2016-7716

FRICTION FACTOR OF SILICON DIOXIDE-WATER COLLOIDAL SUSPENSION FLOW IN CIRCULAR AND SQUARE TUBES

Md. Tanveer Sharif
University of Pittsburgh
Pittsburgh, PA 15213, USA

Sarbottam Pant
Meiden America, Inc.
Northville, MI 48168, USA

Clement C. Tang
University of North Dakota
Grand Forks, ND 58202, USA

ABSTRACT

The present study focuses on the friction factors of a colloidal suspension flow in circular and square tubes. The colloidal suspension was made of silicon dioxide nanoparticles dispersed in distilled water at a concentration of 9.58% by volume. The viscosity and shear stress of the suspension were measured and it was found that the fluid exhibited non-Newtonian behavior. The rheological behavior of the suspension could be adequately modeled as a power-law generalized Newtonian fluid (GNF). When the consistency and the flow behavior indices of the suspension were properly evaluated, the friction factors of the suspension flowing in tubes with circular and square cross-sections exhibited similarities with those of Newtonian fluid flow. In fully-developed laminar flow, the Poiseuille number for the suspension was similar to that for a Newtonian fluid flow. In turbulent flow, the Dodge and Metzner's relations for the friction factor and a generalized Reynolds number can be used to adequately describe the suspension in turbulent flow. Observations from the friction factor measurements showed that the onsets of transition to turbulent flow vary with the cross-sectional shape of the tube and differ from those of Newtonian fluid flow. This might suggest that the cross-sectional shape of the flow passage and the presence of nanoparticles could affect the onset of transition to turbulent flow for the suspension.

INTRODUCTION

Several studies in the past have suggested that the overall thermal conductivity of a fluid can be enhanced by dispersing small particles in a base liquid, such as water and oil [1-3]. The increase in the overall thermal conductivity of the fluid would thereby promote higher heat transfer capability.

In recent years, colloidal suspension containing solid nanoparticles dispersed in liquid base fluids, also known as nanofluids, have received attention for their potential in engineering applications. Several publications have documented that colloidal suspensions can be engineered to be a new class of fluid in heat transfer [4, 5].

Several researchers have documented that by dispersing nanoparticles, such as titanium dioxide (TiO_2), copper oxide (CuO), and aluminum oxide (Al_2O_3) to a liquid base fluid could enhance the overall thermal conductivity of the fluid [6, 7]. Recent investigators have documented beneficial convective heat transfer enhancements using nanofluids [8-10]. However, the increase in thermal conductivity of the fluid does not necessarily mean a beneficial enhancement in the convective heat transfer effectiveness, since there is a tradeoff with having pumping power requirement. The addition of nanoparticles in base liquid would inherently increase the viscous friction of the fluid flow in a system. In addition, the particles in the fluid could bring about potential wear on the system.

In an experimental study conducted by Xuan and Li [11], the friction factors of Cu-water nanofluids flowing in a 10-mm inner diameter tube were roughly the same as those of water for turbulent flow. The Cu-water nanofluids that they used have relatively low particle concentrations, between 1–2% vol. Williams et al. [12] found that the convective heat transfer and friction factor for turbulent flow of alumina-water and zirconia-water nanofluids in tubes can be adequately predicted by existing correlations for single-phase flow.

In laminar flow, the friction factor and convective heat transfer for dispersions, with properly evaluated fluid properties, flowing in tube were found to have no deviation from conventional single-phase flow theory [13]. This finding was documented by Rea et al. [13] for alumina and zirconia dispersed in water, and flowing in a 4.5-mm inner diameter tube. For

nanofluids containing spherical and rod-like nanoparticles, Yu et al. [14] found that conventional single-phase flow theory can satisfactorily predict the friction factors for the nanofluids with spherical particles, but not for those with rod-like particles. They conducted their experimental study in the laminar flow region using Al_2O_3-polyalphaolefin nanofluids with spherical and rod-like nanoparticles [14].

Many of the studies in the literature conducted for the friction factor of colloidal suspensions covered low particle loading, with the nanoparticle concentration in the base liquid at about 5% in volume or lower. At low nanoparticle concentration, the fluids are generally behaving as Newtonian fluid. As the particle loading increases, the fluid rheological behavior could become non-Newtonian. In the present study, SiO_2–water (9.58% vol.) colloidal suspension was used as the working fluid. The SiO_2–water colloidal suspension exhibits the behavior of a non-Newtonian fluid, and it can be modeled as a power-law fluid. Friction factors of the colloidal suspension were measured for circular and square tubes with different hydraulic diameters. The results were then compared with established correlations for Newtonian and non-Newtonian fluids.

BACKGROUND

The Fanning friction factor for internal flow in a circular tube can be defined from the pressure gradient along the tube length as

$$c_f = \frac{1}{2}\left(-\frac{dp}{dx}\right)\frac{D}{\rho V^2} \tag{1}$$

The average fluid velocity (V) in the tube can be determined experimentally by measuring the mass flow rate ($\dot{m} = \rho V A$).

For a laminar fully-developed flow in a circular tube for Newtonian fluids, the conventional theory for friction factor is simply $c_f\, Re = 16$. Incidentally, this friction factor relation is also applicable for non-Newtonian fluids. In a square tube, the friction factor for a laminar fully-developed flow is $c_f\, Re = 14.23$, where the characteristic length for the Reynolds number is the hydraulic diameter, D_h.

When the flow is turbulent, the friction factor for Newtonian fluids can be described using the Blasius [15] correlation, $c_f\, Re^{0.25} = 0.079$, for $4000 \le Re \le 10^5$. There are numerous correlations available in the literature [16-18] that describe the friction factor of turbulent flow in tubes. The friction factor correlation introduced by Churchill [18] is perhaps one of the more elaborate correlations that attempts to span the laminar-to-turbulent regimes:

$$c_f = 2\left[\left(\frac{8}{Re}\right)^{12} + \frac{1}{(A_1 + B_1)^{1.5}}\right]^{1/12} \tag{2}$$

where

$$A_1 = \left\{2.457 \ln\left[\frac{1}{(7/Re)^{0.9} + 0.27(\epsilon/D)}\right]\right\}^{16}$$

and

$$B_1 = \left(\frac{37530}{Re}\right)^{16}$$

In the present study, the effect of wall surface roughness (ϵ) is neglected; hence it is omitted when evaluating A_1.

For a power-law generalized Newtonian fluid, the shear stress and the shearing rate relation is given as

$$\tau = K\left(-\frac{du}{dy}\right)^n \tag{3}$$

where the consistency index (K) and the flow behavior index (n) can be determined experimentally. The flow behavior index describes the fluid behavior, whether it is shear-thinning ($n < 1$) or shear-thickening ($n > 1$). When the fluid is purely Newtonian, the consistency index is equivalent to the dynamic viscosity, and the flow behavior index becomes unity.

When a fluid is modeled as a power-law generalized Newtonian fluid, the friction factor can be described using a generalized Reynolds number, as introduced by Dodge and Meztner [19]:

$$\sqrt{\frac{1}{c_f}} = \frac{4}{n^{0.75}}\ log\left(Re'\, c_f^{1-n/2}\right) - \frac{0.4}{n^{1.2}} \tag{4}$$

where the generalized Reynolds number is defined as

$$Re' = \frac{D^n\, V^{2-n}\, \rho}{8^{n-1}\, K} \tag{5}$$

For a Newtonian fluid ($n = 1$ and $K = \mu$), the generalized Reynolds number becomes the conventional number Reynolds number, $Re = \rho V D/\mu$, for internal flow. In this study, the hydraulic diameter, D_h, for non-circular tube is used in place of the circular tube diameter, D, when evaluating Re and Re'. Hence, the Reynolds number for a square tube is $Re = \rho V D_h/\mu$.

A friction factor plot for Newtonian and non-Newtonian (power-law) fluids using the generalized Reynolds number, as introduced by Dodge and Meztner [19], is illustrated in Figure 1. For a fully-developed laminar flow, both the Newtonian and power-law fluids have the same $c_f\, Re = 16$. In the turbulent flow region, the friction factor curves are influenced by the flow behavior index, n. Once the consistency and the flow behavior indices are known for a fluid, the friction factor can be determined using Figure 1 for a given generalized Reynolds number.

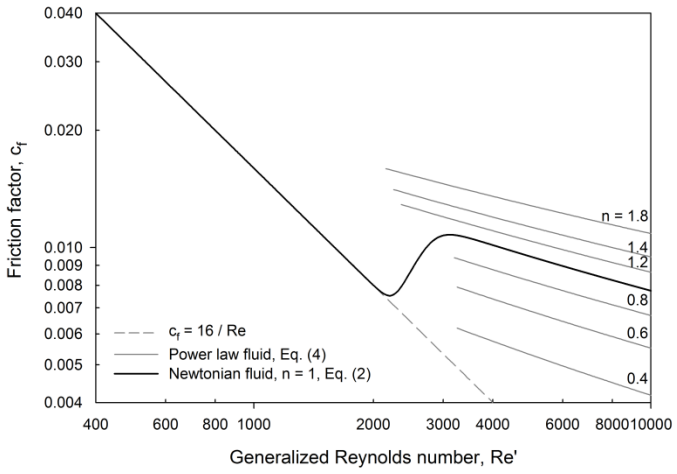

Figure 1. Friction factor for Newtonian and non-Newtonian fluids plotted against the generalized Reynolds number, Re', given by Dodge and Meztner [19]

EXPERIMENTAL APPROACH

Experimental Setup. The overall experimental apparatus utilized for this study is illustrated in Figure 2. The apparatus was designed and built for measuring internal flow characteristics of tubes. The reservoir for storing the working fluid for the experiment is made out of polyethylene with a 3-gallon volume capacity.

A Liquiflo gear pump was used for pumping the working fluid throughout the flow loop. The working fluid was pumped from the reservoir and flowed through a double-tube counter-flow heat exchanger. The heat exchanger kept the flow condition isothermal by removing excess heat that was added during the experiment.

The flow rate of the working fluid was control by a metering valve, and was measured by a Coriolis mass flow meter. The Micro Motion Coriolis mass flow meter measured the flow rate, and the signal from the flow meter was sent to a digital transmitter. The measured flow rate signal from the flow meter is conditioned by the digital transmitter and recorded by the data acquisition system. The accuracy of the Coriolis mass flow meter for a flow range of 1–50 g/s was ±0.1%. The working fluid exiting the Coriolis mass flow meter is flowed to the test section.

The pressure difference between the inlet and exit of the test section was measured by Rosemount pressure transmitters. There were three pressure transmitters with each covering different gage pressure ranges up to 62, 248, and 2070 kPa. The accuracy of the pressure transmitters is within ±0.15%. At the test section inlet and exit, the bulk temperatures of the working fluid were measured with T-type thermocouples. The inlet and exit temperatures of the working fluid would be used for the evaluation of the fluid properties. In addition, the temperatures would be used for validation that the flow condition for the experiment was isothermal. The output signals from the flow meter, pressure transmitters and the thermocouples were recorded using an Agilent data acquisition system.

In the present study, brass C260 tubes with circular and square cross-sections were used as the test sections. The hydraulic diameters for the tubes used in this study were 0.876, 1.71, and 2.46 mm. Each tube has a length-to-diameter ratio of 100. Optical microscopy was used to verify the cross-sectional dimensions of the tubes. Small segments of each tube cross section were analyzed using a Zeiss LSM confocal microscope. The microscopy analysis has determined that the uncertainty of the inner hydraulic diameters was about ±1% at 95% confidence level using the Student's *t*-distribution.

Colloidal Suspension Properties. The colloidal suspension used in this study contained SiO_2 nanoparticles (9.58% vol.) dispersed in a base liquid of water. The colloidal suspension was manufactured by Alfa Aesar®, and the SiO_2 particles have an average particle size of 50 nm. The rheological behavior of the colloidal suspension was characterized by Brookfield DV3T coaxial cylinder rheometer. The colloidal suspension shear stresses and shearing rates were measured for temperatures between 7 and 60°C. During the measurements, the temperature of the colloidal suspension was maintained using a Brookfield temperature bath. The shear stress, shearing rate, and temperature data obtained for the measurements were used to determine the consistency and the flow behavior indices of the colloidal suspension.

Experimental Uncertainty. The friction factor can be evaluated from the measurements of the inner hydraulic diameter (D), the test section length (L), the mass flow rate ($\dot{m}$), the pressure drop (Δp) across the test section, and the working fluid density (ρ). Each of these measured parameters has a quantifiable uncertainty associated with it, as summarized in Table 1. In estimating the experimental uncertainties for the measured friction factors, the procedures described by Kline and McClintock [20] and Moffat [21] were used. The estimated experimental uncertainties associated with the measured friction factors were determined to be between ±5.5 and ±8.5%. The uncertainty of the inner hydraulic diameter of the tube contributed the most to the uncertainties of the friction factors.

Table 1. Summary of the estimated experimental uncertainties

Measured parameters	Uncertainty, %
Inner diameter, D	±1.0
Length between pressure taps, L	±0.6
Mass flow rate, $\dot{m}$	±0.2
Pressure drop, Δp	±0.2
Density, ρ	±1.5
Friction factor, c_f	±5.5 to ±8.5

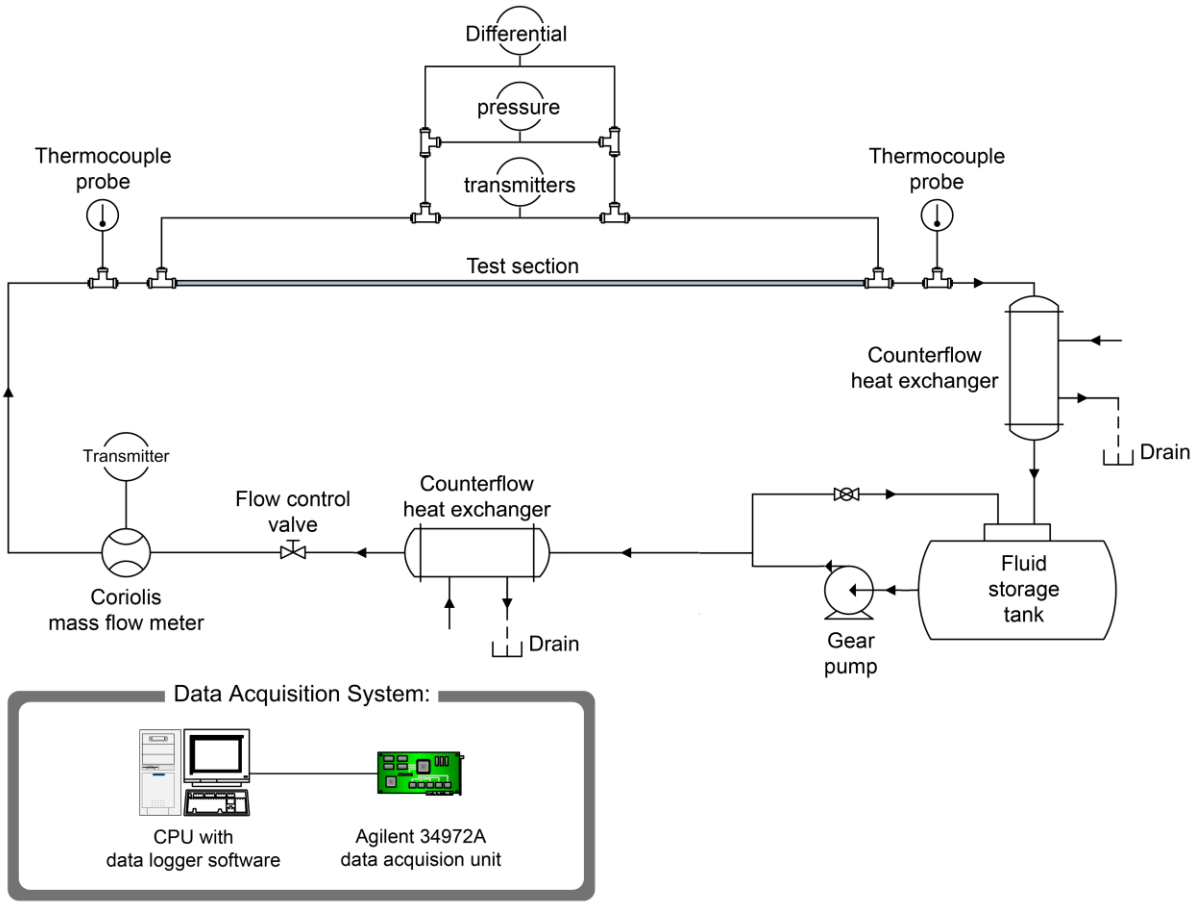

Figure 2. Experimental setup schematic for colloidal suspension flow pressure drop measurements

EXPERIMENTAL RESULTS

Rheological Behavior of SiO_2–Water. The rheological behavior of the SiO_2–water (9.58% vol.) colloidal suspension was characterized at different temperatures. The fluid is modeled as a power-law fluid. With the measured results that included the shear stresses, shearing rates, and temperatures, the indices for the fluid consistency and the flow behavior were determined. Figure 3 shows the effect of temperature on the fluid consistency index, from 7 to 60°C. The consistency index of the SiO_2–water colloidal suspension begins from 2.8 mPa·s^n at 7°C and decreases with increasing temperature to 0.08 mPa·s^n at 60°C.

The flow behavior index of the SiO_2–water (9.58% vol.) colloidal suspension is also influenced by temperature. Figure 4 illustrates the response of the flow behavior index of the fluid to temperature variation from 7 to 60°C. The flow behavior index of the colloidal suspension starts from a value of 1.03 at 7°C and increases with increasing temperature to a value of 1.61 at 60°C.

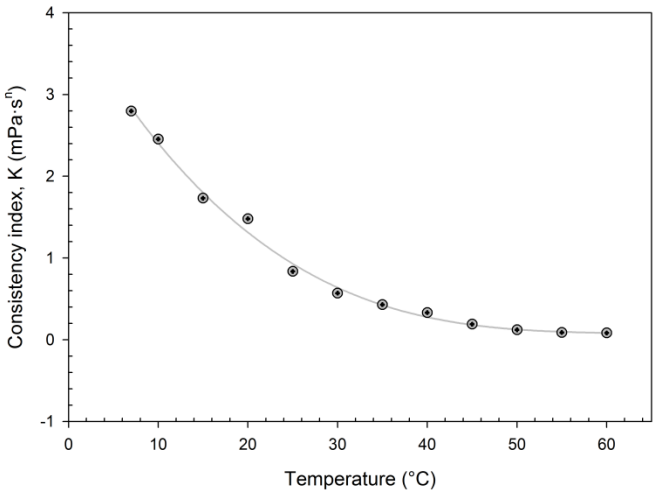

Figure 3. The consistency index of SiO_2–water (9.58% vol.) colloidal suspension plotted against temperature

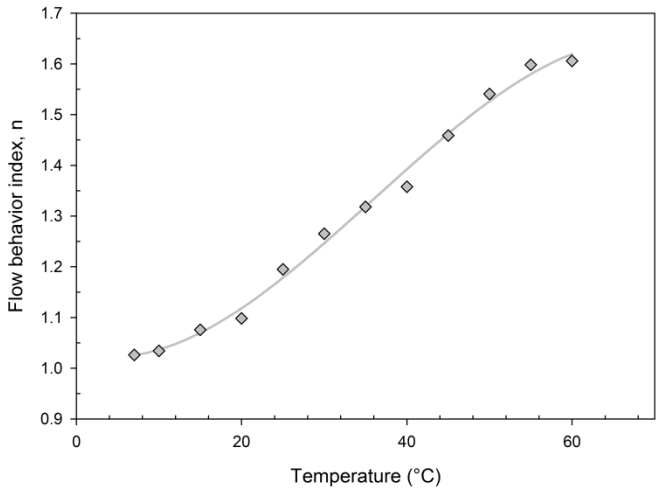

Figure 4. The flow behavior index of SiO_2–water (9.58% vol.) colloidal suspension plotted against temperature

Friction Factor of Water Flow. Before conducting friction factor measurements for the SiO_2–water (9.58% vol.) colloidal suspension flow, the friction factors for water flow in a circular tube were measured. This procedure was to validate that the experimental setup could be used to duplicate friction factor results that have been established in the literature. The friction factor measurements for water flow were conducted from a Reynolds number of approximately 400 to 8700. The measurements were conducted for a circular tube with an inner diameter of 2.46 mm.

The results measured for the water flow friction factor were compared with the friction factor evaluated from correlations available in the literature. For laminar fully-developed flow, the measured friction factors were compared with $c_f\, Re = 16$. For Reynolds number greater than 4000, the measured friction factors were compared with $c_f\, Re^{0.25} = 0.079$, the Blasius [15] correlation, see Figure 5.

When the measured friction factors for water flow were compared with the established friction factor correlations, the agreement between them was within ±5% agreement. The discrepancies between the measured and calculated values were within the estimated experimental uncertainties.

Friction Factor of SiO_2–Water Flow. The friction factor results for SiO_2–water (9.58% vol.) colloidal suspension flow were measured for both circular and square tubes. For both circular and square tubes, measurements were conducted for three different hydraulic diameters, 0.876, 1.71, and 2.46 mm.

For the SiO_2–water colloidal suspension flow in a 2.46-mm-diameter circular tube, the friction factors in the laminar region agrees with the friction factors of water. Both Newtonian and non-Newtonian fluids exhibit friction factors that can be described by $c_f\, Re = 16$. The friction factors for both SiO_2–water colloidal suspension and water are in good agreement from a Reynolds number of about 400 to 2800, see Figure 6.

When the Reynolds number is above 2800, the friction factors of the colloidal suspension diverge from the friction factors of water and continue until they converge with the line predicted by the Dodge and Meztner [19] correlation, Eq. (4), for n = 1.2 at $Re' \approx 4700$.

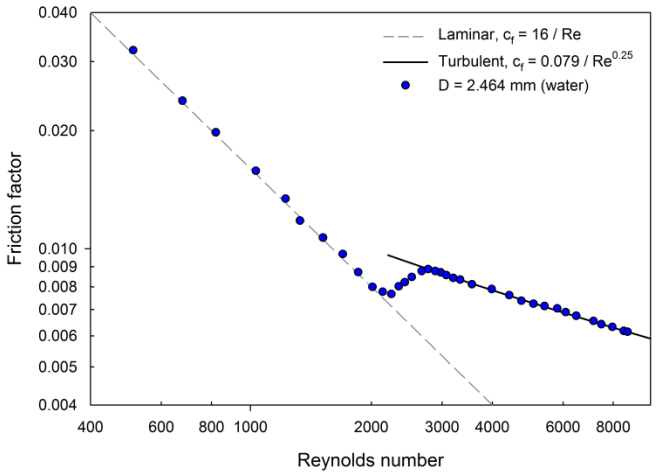

Figure 5. Measured friction factors of water flow in a 2.46-mm-diameter circular tube in comparison with $c_f\, Re = 16$ for laminar flow and the Blasius [15] correlation for turbulent flow

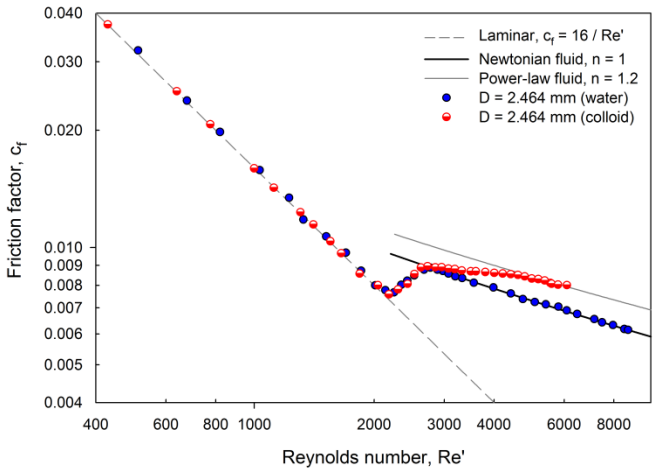

Figure 6. Measured friction factors of water and SiO_2–water (9.58% vol.) colloidal suspension flow in circular tube of D = 2.46 mm in comparison to the predictions of Eq. (4)

The friction factors of the SiO_2–water colloidal suspension flow in circular tubes of different diameters were measured and plotted in Figure 7. In the laminar flow region, the friction factors for all three tubes agree with $c_f\, Re = 16$. However, the friction factor for the onset of transition to turbulent flow varies with the tube diameter. As the tube diameter decreases, the friction factor starts to depart from the $c_f\, Re = 16$ curve at lower Re' value. As the tube diameter increases, the departure of the

friction factor from the $c_f\ Re = 16$ curve occurs at slightly higher Re'.

The friction factors of the SiO_2–water colloidal suspension flow in square tubes of different hydraulic diameters were measured and plotted in Figure 8. For SiO_2–water colloidal suspension flow in square tubes, the friction factors in the laminar flow region agree with $c_f\ Re = 14.23$. The friction factors in the transition to turbulent flow region were measured to be higher for tube with lower hydraulic diameter.

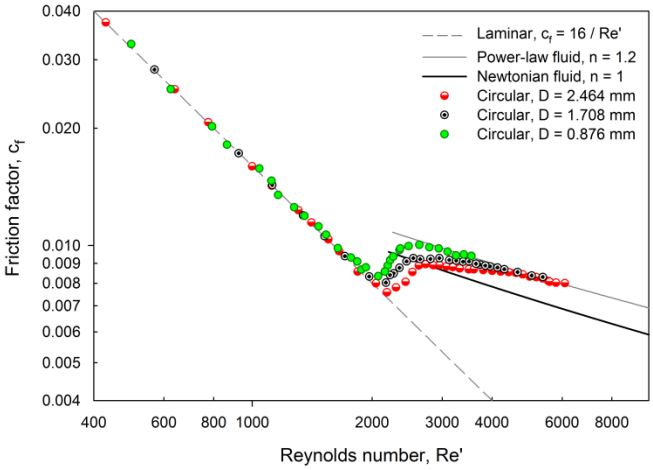

Figure 7. Measured friction factors of SiO_2–water (9.58% vol.) colloidal suspension flow in circular tubes of different diameters in comparison to the predictions of Eq. (4)

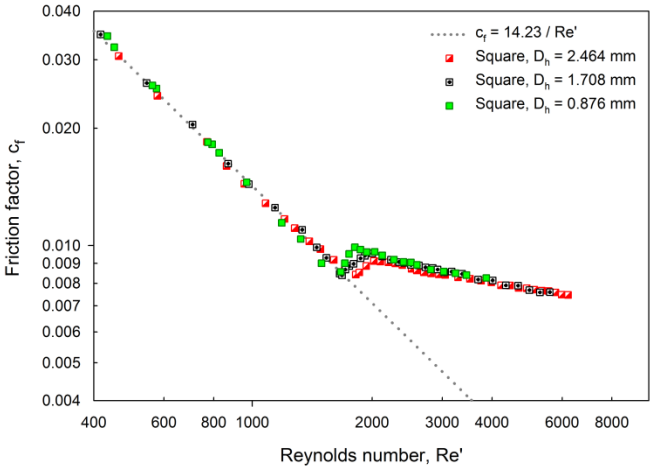

Figure 8. Measured friction factors of SiO_2–water (9.58% vol.) colloidal suspension flow in square tubes of different hydraulic diameters

Figure 9 shows the friction factors of SiO_2–water colloidal suspension flow measured for circular and square tubes at an equivalent hydraulic diameter of 2.46 mm. At the laminar and turbulent flow regions, the friction factors for square tube are lower than the friction factors for circular tube.

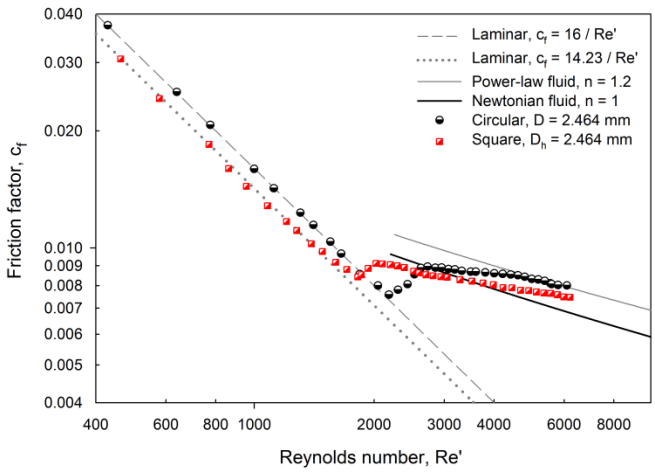

Figure 9. Comparison of the measured friction factors for SiO_2–water (9.58% vol.) colloidal suspension flow in circular and square tubes with $D = D_h = 2.46$ mm

SUMMARY

The results obtained in this study indicated that the SiO_2–water (9.58% vol.) colloidal suspension can be adequately modeled as a power-law fluid. The consistency and flow behavior indices are affected by temperature.

In the fully-developed laminar flow region, the friction factors for both circular and square tubes have similar friction factors of a Newtonian fluid, where $c_f\ Re$ for circular and square tubes are 16 and 14.23, respectively. For circular tubes in the turbulent flow region, the friction factors of colloidal suspension can be adequately described by the relation given by Dodge and Meztner [19].

The friction factor for the onset of transition to turbulent flow in circular tube varies with the tube diameter. As the circular tube diameter decreases, the friction factor departs the laminar friction factor curve at lower Reynolds number.

In square tubes, the colloidal suspension friction factors in the transition region were observed to be influenced by the tube hydraulic diameter. When compared with a circular tube, the friction factors for square tube are lower than the friction factors for circular tube in both the laminar and turbulent flow regions, with the exception of the transition region.

ACKNOWLEDGMENTS

Part of this work was sponsored by funds from the North Dakota NASA EPSCoR and the University of North Dakota, Mechanical Engineering Department. The views expressed in this article are those of the authors and do not reflect the official policy or position of the North Dakota NASA EPSCoR. The authors would also like to acknowledge Emerson Rosemount for generously donating the pressure transmitters utilized in this study.

NOMENCLATURE

A	cross-sectional area, m^2
c_f	Fanning friction factor
D	inside diameter, m
D_h	hydraulic diameter ($= 4A/P$), m
du/dy	shearing rate, s^{-1}
K	fluid consistency index
L	length between pressure taps, m
n	flow behavior index
$\dot{m}$	mass flow rate, kg/s
P	wetted perimeter, m
p	pressure, Pa
x	spatial coordinate along tube/channel length, m
Re	Reynolds number ($= \rho VD/\mu$)
Re'	generalized Reynolds number
V	average flow velocity, m/s

Greek symbols

ϵ	wall surface roughness, m
μ	dynamic viscosity, Pa·s or cP
ρ	density, kg/m^3
τ	shear stress, Pa

REFERENCES

[1] Hamilton, R. L., and Crosser, O. K., 1962, "Thermal Conductivity of Heterogeneous Two Component Systems," Industrial and Engineering Chemistry Fundamentals, 1, pp. 187–191.

[2] Ahuja, A. S., 1975, "Augmentation of Heat Transport in Laminar Flow of Polystyrene Suspensions. I. Experiments and Results," Journal of Applied Physics, 46, pp. 3408–3416.

[3] Ahuja, A. S., 1975, "Measurement of Thermal Conductivity of (Neutrally and Nonneutrally Buoyant) Stationary Suspensions by the Unsteady-State Method," Journal of Applied Physics, 46, pp. 747–755.

[4] Masuda, H., Ebata, A., Teramea, K., and Hishinuma, N., 1993, "Alteration of Thermal Conductivity and Viscosity of Liquid by Dispersing Ultra-Fine Particles," Netsu Bussei, 7, pp. 227–233.

[5] Choi, S. U. S., 1995, "Enhancing Thermal Conductivity of Fluids with Nanoparticles," D. A. Siginer and H. P. Wang, eds., Proceedings of the 1995 ASME International Mechanical Engineering Congress and Exposition, Fluids Engineering Division, San Francisco, CA, 231, pp. 99–105.

[6] Prasher, R., Bhattacharya, P., and Phelan, P. E., 2005, "Thermal Conductivity of Nanoscale Colloidal Solutions (Nanofluids)," Physical Review Letters, 94, p. 025901.

[7] Wang, X.-Q., and Mujumdar, A. S., 2007, "Heat Transfer Characteristics of Nanofluids: A Review," International Journal of Thermal Sciences, 46, pp. 1–19.

[8] Yang, Y., Zhang, Z. G., Grulke, E. A., Anderson, W. B., and Wu, G., 2005, "Heat Transfer Properties of Nanoparticle-in-Fluid Dispersions (Nanofluids) in Laminar Flow," International Journal of Heat and Mass Transfer, 48, pp. 1107–1116.

[9] Fotukian, S. M., and Nasr Esfahany, M., 2010, "Experimental Investigation of Turbulent Convective Heat Transfer of Dilute γ-Al_2O_3/Water Nanofluid inside a Circular Tube," International Journal of Heat and Fluid Flow, 31, pp. 606–612.

[10] Heyhat, M. M., Kowsary, F., Rashidi, A. M., Momenpour, M. H., and Amrollahi, A., 2013, "Experimental Investigation of Laminar Convective Heat Transfer and Pressure Drop of Water-Based Al_2O_3 Nanofluids in Fully Developed Flow Regime," Experimental Thermal and Fluid Science, 44, pp. 483–489.

[11] Xuan, Y., and Li, Q., 2003, "Investigation on Convective Heat Transfer and Flow Features of Nanofluids," ASME Journal of Heat Transfer, 125, pp. 151–155.

[12] Williams, W., Buongiorno, J., and Hu, L.-W., 2008, "Experimental Investigation of Turbulent Convective Heat Transfer and Pressure Loss of Alumina/Water and Zirconia/Water Nanoparticle Colloids (Nanofluids) in Horizontal Tubes," ASME Journal of Heat Transfer, 130, p. 042412.

[13] Rea, U., McKrell, T., Hu, L.-W., and Buongiorno, J., 2009, "Laminar Convective Heat Transfer and Viscous Pressure Loss of Alumina-Water and Zirconia-Water Nanofluids," International Journal of Heat and Mass Transfer, 52, pp. 2042–2048.

[14] Yu, L., Liu, D., and Botz, F., 2012, "Laminar Convective Heat Transfer of Alumina-Polyalphaolefin Nanofluids Containing Spherical and Non-Spherical Nanoparticles," Experimental Thermal and Fluid Science, 37, pp. 72–83.

[15] Blasius, H., 1913, "Das Ähnlichkeitsgesetz bei Reibungsvorgängen in Flüssigkeiten," Forschungsarbeiten auf dem Gebiete des Ingenieurwesens, 131, pp. 1–40.

[16] Drew, T. B., Koo, E. C., and McAdams, W. H., 1932, "The Friction Factor for Clean Round Pipes," Trans. AIChE, 28, pp. 56–72.

[17] Bhatti, M. S., and Shah, R. K., 1987, "Turbulent and Transition Flow Convective Heat Transfer in Ducts," in *Handbook of Single-Phase Convective Heat Transfer*, S. Kakaç, R. K. Shah and W. Aung, eds., John Wiley & Sons, New York, pp. 4.1–4.166.

[18] Churchill, S. W., 1977, "Friction-Factor Equation Spans All Fluid-Flow Regimes," Chemical Engineering, 84, pp. 91–92.

[19] Dodge, D. W., and Metzner, A. B., 1959, "Turbulent Flow of Non-Newtonian Systems," AIChE Journal, 5, pp. 189–204.

[20] Kline, S. J., and McClintock, F. A., 1953, "Describing Uncertainties in Single-Sample Experiments," Mechanical Engineering, 75, pp. 3–8.

[21] Moffat, R. J., 1988, "Describing the Uncertainties in Experimental Results," Experimental Thermal and Fluid Science, 1, pp. 3–17.